International Journal of Engineering Research
Volume No.6, Issue No.1, pp :11-17

ISSN:2319-6890 (online),2347-5013(print)
1 Jan. 2017

Correlation of Effect of Plasma-Nitridingon Fatigue Life of Low-Alloy Steel with Surface Stresses Estimated using FEM Analysis

U. N. Puntambekar[1], V. B. Patel[2], G. S. Grewal[3] , P. B. Joshi[4]
[1,2]Technology Center, Electrical Research & Development Association, Vadodara, India
[3]Mechanical & Insulating Materials Division, Electrical Research & Development Association, Vadodara, India
[4]Metallurgical and Materials Engineering Dept., M. S. University of Baroda, Vadodara, India
uday.puntambekar@erda.org

Abstract :Surface treatments affect fatigue life of rotating components due to stresses induced on surface. The fatigue life can be correlated with the stresses induced. However, to measure stresses in actual practice is time-consuming as well as costly process. Alternatively, FEA studies are carried-out to determine the stresses induced. In this investigation plasma nitriding has been carried-out to enhance surface related properties of steel components. The hardened case in these components comprise of a compound (white) layer on top followed by a diffusion zone underneath it. The increase in hardness and strength at the surface leads to improvement in fatigue life. However, increase in thickness of the compound layer beyond a certain critical reduces the fatigue life of the base material. Hence, it is desirable to have close control on the process to limit the formation of excessively thick compound layer. This paper discussesthe effect of thickness of white (compound layer) on fatigue life of component. The stresses induced due to plasma nitriding were determined by Finite Element Analysis (FEA)on the plasma nitrided samples with respect to thickness of compound layer for the En-24 steel. The rotating bending fatigue test on plasma nitrided samples was conducted at various stress levels to plot S-N curves. The experimental data indicates that the fatigue life of samples increases up to a certain thickness of compound layer and then decreases. This finding has been correlated with the stresses induced using FEA.

Keywords : FEA, White layer, Plasma nitriding, Fatigue

I. Introduction

The plasma nitriding is one of the thermo-chemical processes used to harden the surface of steel. Similar to other nitriding processes, plasma nitriding also enhances the surface related properties such as wear & erosion resistance as well as fretting & plain fatigue strength ([i], [ii]).
In general, the fatigue strength depends upon the strength level of surface layer. There are three ways in which the surface treatment influences fatigue strength; firstly, by affecting the intrinsic fatigue strength of material at the surface, secondly by introducing or removing residual stresses in the surface layers and thirdly, by introducing or removing irregularities in the surface which act as stress raisers [iii]. Plasma nitriding enhances fatigue strength by first two mechanisms stated above. Relationships have also been established between the case properties and fatigue strength [iv].

Finite Element Analysis or Method (FEA or FEM) is a tool used for solving engineering problems through modeling and simulation. FEA is extensively used for stress and fatigue analysis of dynamically loaded components [v-ix].

Components subjected to surface treatments are most likely to initiate fatigue cracks at surface. Hence, stress pattern developed at and near surface are required to be established using simulation methods. Usually the surface treatments generate residual stresses in the surface [xi-xvi]. FEM tool is used to determine residual stresses of components subjected to thermal, thermo-mechanical and mechanical treatments [ix].

At the same time, state of stress in the surface layer, while it is subjected to loading, will change the stress pattern already existing due to residual stresses [xvii-xxi].

However, for determining stress state using FEA, availability of precise data on mechanical properties of phases present in the surface is important. Also, results of such analysis done have to be validated before it is used for actual application. Compound (white) layer in the plasma nitrided components comprises of various types of nitrides (ε-nitrides & γ'-nitrides) which have different mechanical properties. Hence, the response of such layers to the loading will vary depending on the phases present. Plasma nitrided components have not been studied for state of stress developed in the compound layers of varying phases. Using the property related data available on various nitrides steels [xviii & xxii] it is possible to determine the effective state of stress in the compound layer and then correlate with the experimental results of fatigue testing.

In this work an attempt has been made to modify the surface characteristics of the hardened & tempered AISI 4340 steel specimens subjected to plasma nitridingand to examine their effect on fatigue behavior of this steel. The methodology of smooth bar rotating bending fatigue testing, using a R. R. Moore type rotating bending fatigue testing machine is adopted for evaluating the fatigue behavior after respective surface treatments. The surface treated specimens were characterized for coating thickness, surface hardness and/or hardness profile, phase identification using XRD, optical and SEM fractography and microstructure. The results of fatigue test have been correlated with compound layer thickness values and the same has been validated using Finite Element Analysis (FEA) approach.

II. Material and Methodology

ISSN:2319-6890 (online),2347-5013(print)
1 Jan. 2017

a) Specimen Design and Fabrication:
AISI4340 grade low-alloy steel, which is a most commonly used shafting material, has been selected for this study. A coil of hot-rolled wire-rod of 20 mm diameter was obtained from steel plant. Subsequently wire drawing was done to obtain scale and decarburization free rods of 18.7 mm diameter. The rod material had an average prior austenite grain size No. 6 (as per ASTM E – 115) and controlled non-metallic inclusions index equal to 1.5 as per IS: 4163 – 2004.Figure 1 shows the schematic of the test sample used for fatigue testing, wherein the gauge diameter of 12 mm contains a machined, semi-circular notch of depth 1.5 mm and root radius of 1 mm. This translates into a stress concentration factor of 2, as computed using analytical elastic stress analysis theory. The normalized wire-rods were given hardening & tempering heat-treatment by preheating at 500˚C,austenitising at 855˚C, quenching in oil & finally tempering at 520˚C to obtain hardness of 32±2 HRC (≅ 320 HV).

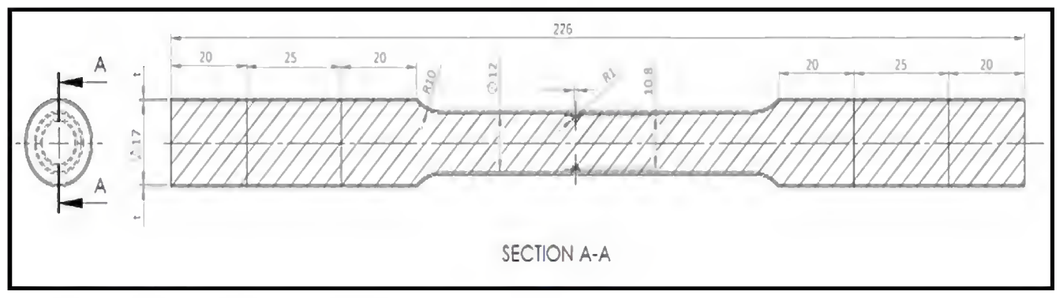

Fig. 1: Schematic of the fatigue test specimen

b) Surface Treatment – Plasma Nitriding:
The machined fatigue test samples were subjected to plasma nitriding to obtain three different thicknesses (categories) of compound (white) layer i.e. without compound layer (category-1), with compound layer thickness of up to 10 microns (category-2) and thickness of > 10 microns (category-3). For all these categories of samples, the nitrided layer thickness was around 400 microns.

c) Fatigue Testing:
The rotating bending fatigue tests were conducted, using a R. R. Moore type rotating bending fatigue testing machine. The samples without surface treatment (Control category), and surface-treated categories (3 nos. each) were evaluated for fatigue life. Six stress levels with four replications were selected for fatigue evaluation.

d) Finite Element Analysis (FEA):

To rationalize the key finding of this study, namely that white layer thickness below 10 µm does not degrade the fatigue life while white layer thickness of greater than 10 µm results in reduction in fatigue life to a value below the threshold fatigue life of the base material, it is pertinent to note that X-ray diffraction analysis clearly indicates that the constitution of the white layer for thickness below 10 µm is predominantly Fe_4N while for thickness greater than 10 µm it is $Fe_{2-3}N$. Since the elastic constants of the $Fe_{2-3}N$ and Fe_4N are significantly different, it is reasonable to conjecture that the magnitude of the state of stress in white layers with predominant $Fe_{2-3}N$ and Fe_4N phase constitution respectively may be significantly different in comparison to the base material under identical external loading conditions. Demonstration of existence of such differences in the state of stress in the two types of white layers will then open-up possibility of direct correlation of the stress state in the white layer with the observed behavior of the fatigue life as a function of thickness of the white layer.

For this purpose, recourse was taken to static elastic stress analysis in the isotropic solid approximation. This analysis was conducted in the following sequence:

i. Explicit 3D model of a reduced section of the fatigue specimen is preparing using Solid Works package.
ii. Formulation and solution of a closed form analytical solid mechanics model of the "Composite beam" fatigue specimen using a tractable geometrical approximation for the purpose of validation of the FEM results.
iii. Meshing of the Solid Works generated 3D model after importing into FEM based structural analysis package of ANSYS.
iv. Stress state solution using steady state elastic analysis.
v. Comparison of results with the closed form solution obtained in step ii, above for the purpose of validation of the FEM analysis.
vi. Tuning of the FEM model and determination of stress state as a function of white layer thickness for white layers of Fe_4N & $Fe_{2-3}N$ constitution.

FEM software ANSYS 15.0 was used for modeling, meshing, as well as stress analysis. Properties were assigned to materials including base material and coatings. Boundary conditions were applied on the specimen for load & displacement (constraints). Output parameters (plots) in terms of stresses generated (Max. normal stresses) were obtained. The stress values were correlated with behavior observed during fatigue testing.

A 3D solid model of the relevant portion of the fatigue specimen was developed in Solid Works package and a number of such models were replicated using various thicknesses of white layer ranging from 5 µm to 20 µm. A 3D CAD drawing of full size fatigue test specimen is shown in Fig. 2.

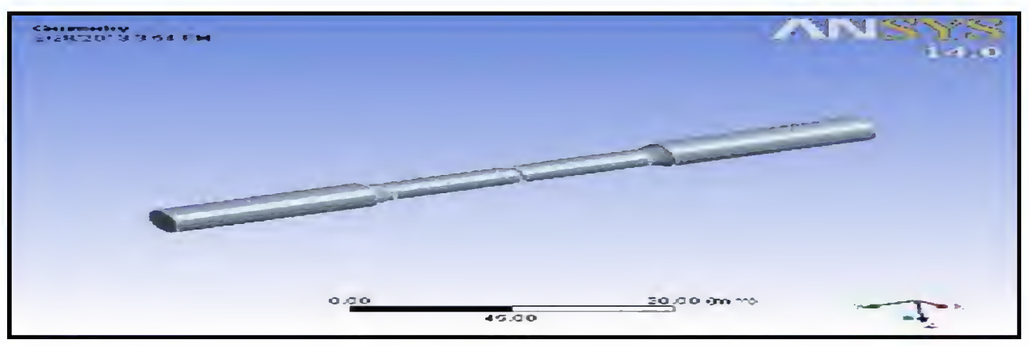

Fig. 2: 3-D drawing of the full size fatigue test specimen

The following cases were considered for FEM analysis of the fatigue specimen. Stress analysis was done for a case of bending moment of 5000 Nmm.

Table 1: Geometry configurations considered for analysis

Case	Compound layer configuration	
	Thickness of Fe_4N Layer, µm	Thickness of $Fe_{2-3}N$ Layer, µm
I	5, 10, & 20	Nil
II	Nil	5, 10, & 20
III	10	5
IV	10	10

ISSN:2319-6890 (online),2347-5013(print)
1 Jan. 2017

Table 2: Properties assigned to the base material & phases in compound layer

Material / Phase in compound layer	Properties	
	Young's modulus *E*,GPa	Poisson's ratio *v*
Base material	210	0.30
γ'-Fe_4N	162	0.36
ε-$Fe_{2-3}N$	243	0.29

The representative 3-D models, meshed model and models with boundary conditions applied are shown for each case in the Fig. 3 to 5.

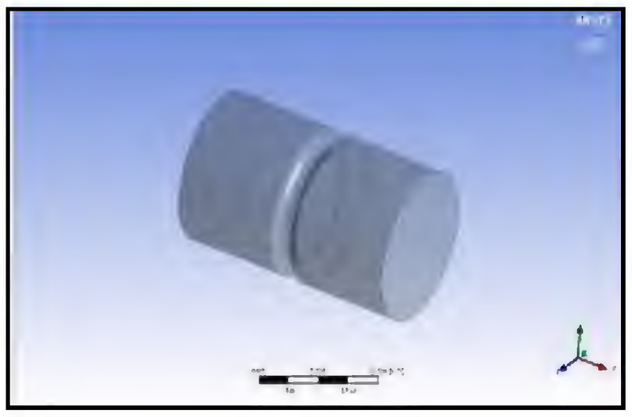

(a)

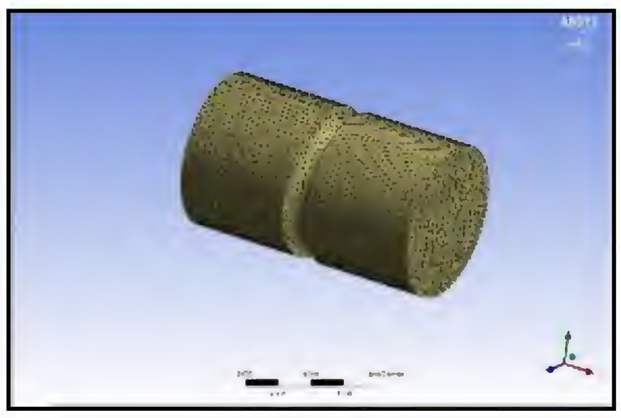

(b)

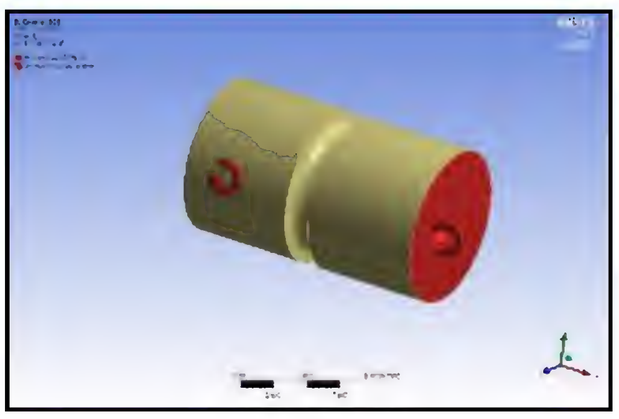

(c)

Fig. 3: FEM Modeling For Analysis of Untreated Specimen (a) 3-D CAD Model (b) Meshed Model and (c) Model With Boundary Conditions

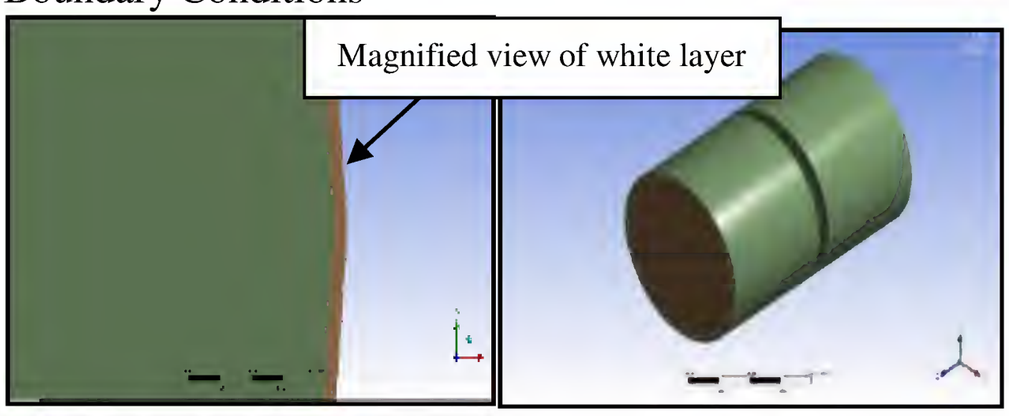

(a)

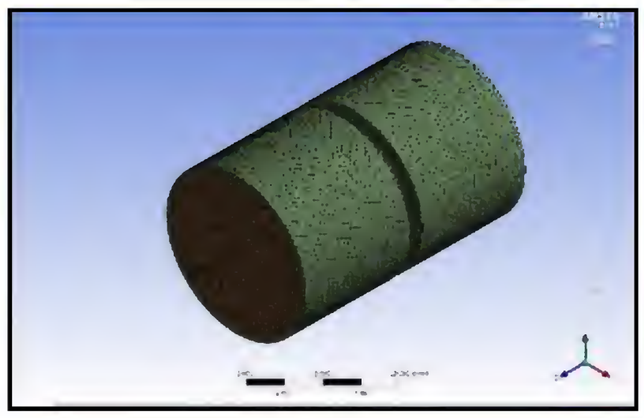

(b)

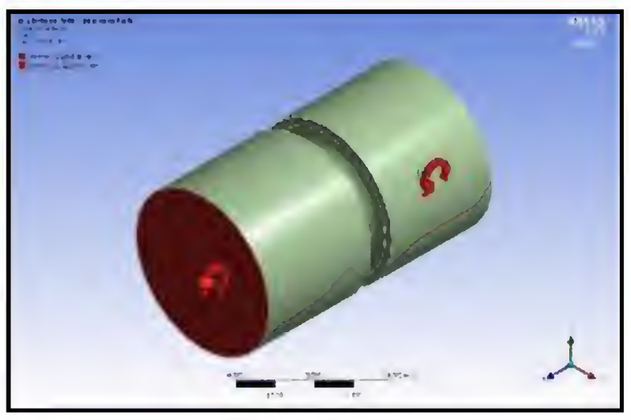

(c)

Fig. 4: FEM modeling for analysis of Fe_4N layer (a) 3-D CAD model (b) Meshed model and (c) Model with boundary conditions

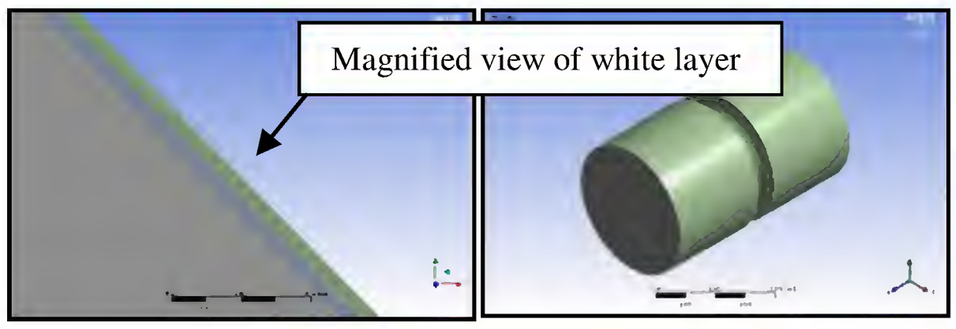

(a)

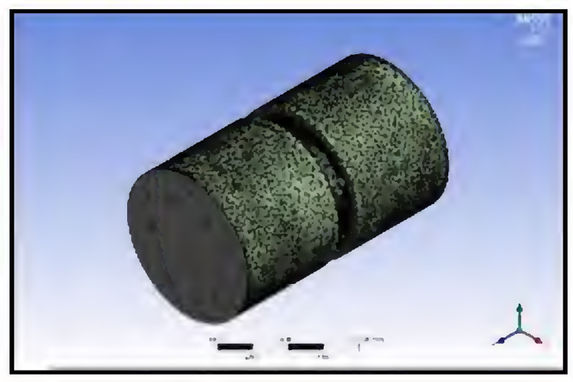

(b)

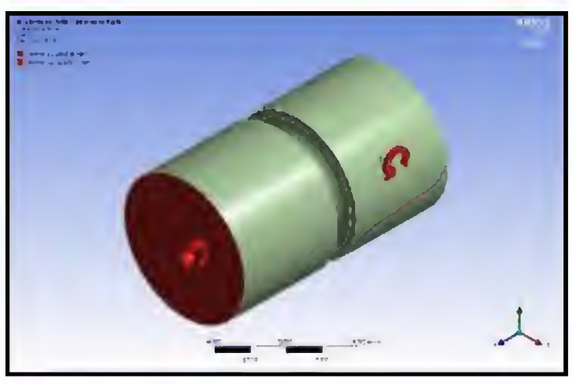

(c)

Fig. 5: FEM Modeling for Analysis of Composite Fe_4N &Fe_{2-3}NWhite Layer (a) 3-D CAD Model (b) Meshed Model and (c) Model with Boundary Conditions

Validation of FEM Analysis Procedure Using Closed Form Equivalent Composite Beam:

For the purpose of validating the FEM analysis procedure, a composite beam as shown in Fig. 6 with neutral axis X-X was considered.

ISSN:2319-6890 (online),2347-5013(print)
1 Jan. 2017

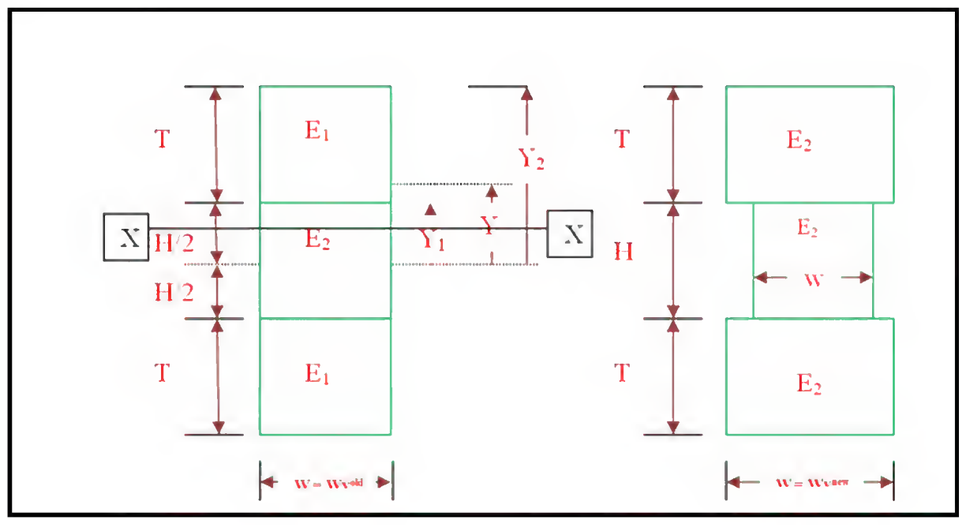

(a) (b)

Fig. 6: Composite Beam Considered for Validation Purpose
(a) Original "Actual" Cross Section and (b) Transformed Cross Section

Nomenclatures used -

- Subscript "1" corresponds to white layer
- Subscript "2" corresponds to base material
- "W" is width and "T" is the thickness of the composite beam
- E1, E2 and E are elastic constant for white layer, base material and composite, respectively
- X-X is Neutral axis

With reference to Fig. 6, to enable the application of elementary "monolithic" beam theory, we need to convert the composite "E_1-E_2" cross-section into a monolithic E_2 (based material) cross-section. It can be shown that this can be accomplished by the following algorithm:

a) For every $y_1 \leq y \leq y_2$,

Change beam width W_y^{old} to new beam width W_y^{new} by transformation:

$$W_y^{new} = (E_1/E_2)\left(W_y^{old}\right)$$

b) The neutral axis of this equivalent beam will now coincide with its centroidal axis. Thus, we can compute section stress, σ_{zz}^{Equiv} by the flexural expression:

$$\sigma_{zz}^{Equiv} = -M_{xx}\,Y/I_{xx}^{Equiv}$$

Where,
M_{XX}= Bending moment
Y= Outer fibre distance from neutral axis
I_{XX}= Area moment

c) Next we need to normalize the equivalent stress, σ_{zz}^{Equiv} to actual stress in original composite beam by:

$$\sigma_{zz}^{actual} = \left(E_2^{actual}/E_1^{transformed}\right)\left(\sigma_{zz}^{Equiv}\right)$$

$$= (E_1/E_2)\left(\sigma_{zz}^{Equiv}\right)$$

In the present work, the above formulation has been used to compute the state of stress distribution in a rectangular cross-section beam by approximating the beam height to be equal to the diameter of the specimen.

III. Results and Discussion

The analysis of composite beam was carried out as mentioned above and also using FEM software "ANSYS -Version 15.0". Data used for both these analyses is given in Table 3. These comparisons are presented in Table 4. Close fit was found between the FEA and closed forms solutions. Hence, it can be said that the FEA procedure used is validated.

Table 3. Data used for Composite Beam Analysis

Parameters	Values
Thickness of base material, (mm)	25
Width of base material, (mm)	10
E_1 for coating, (GPa)	72
E_2 for Base material, (GPa)	207
IXX (base material), (mm4)	13020.8
σ_{XX} (monolithic), (N/mm^2)	4.8
Moment, (Nm)	5

Table 4. Results of Composite Beam Analysis

Thicknesof coating (mm)	Width of coating (new) (mm)	I_{XX} (mm^4)	σ_{XX} (transformed) N/mm^2	Calculated σ_{XX} (composite) (N/mm^2)	σ_{XX} (composite) (max) (N/mm^2) obtainedthrough FEA
5.000	3.478	20919	3.59	1.454	1.45
2.000	3.478	15561	4.34	1.623	1.62
1.000	3.478	14197	4.58	1.653	1.67
0.500	3.478	13586	4.69	1.664	1.68
0.250	3.478	13298	4.75	1.667	1.69
0.100	3.478	13130	4.78	1.668	1.73
0.050	3.478	13075	4.79	1.669	1.71
0.025	3.478	13048	4.79	1.669	1.70

FEM Analysis on Actual Fatigue Geometry:

A sub section of the fatigue specimens was modeled in SOLID WORKS 3D modeling package. This model was subsequently

ISSN:2319-6890 (online),2347-5013(print)
1 Jan. 2017

imported in to ANSYS version 15.0 FEM software and subjected to linear elastic-isotropic-stressanalysis.

Typical output plots of this analysis are presented in Fig. 7 to Fig. 10. The results of elastic analysis are summarized in Tables 5 to 7 and are also summarized in Fig. 11 to 12.

In Fig. 11, plots for maximum normal fiber stress in Fe_4N and Fe_3N are compared as a function of white layer thickness varying from 5 µm to 20 µm. It can be noted from these plots that the peak stress in the $Fe_{2-3}N$ phase is nearly 50% higher than in the Fe_4N phase. Further, it is also pertinent to note that significant variations in the value of the peak stress as a function of white layer thickness do not exist for both phases. This lack of significant variation is essentially associated with the low thickness of the white layer.

In Fig. 12, plot of the state of maximum normal fiber stress is presented in the actual plasma nitrided fatigue specimen as a function of the thickness in the white layer from the surface of the base material. When we compare this plot with the peak normal stress in the base material, it is found that up to a distance of 10 µm in white layer the peak normal fiber stress is about 25% lower than the peak normal fiber stress in the base material. However, beyond a distance of 10 µm, the stress in the white layer rapidly switches over to a value which is nearly 30% higher than the peak normal fiber stress in the base material. The zone of "switching over" of the normal stress isdue to presence of a two phase white layer zone of $Fe_4N + Fe_{2-3}N$.

Further, it is has been found that the post- plasma nitriding residual stress in the white layer of $Fe_{2-3}N$ constitution is of tensile orientation while that in the Fe_4N phase is of compressive orientation. Thus, presence of tensile normal stress in the $Fe_{2-3}N$ layer, (in white layer with thickness greater than 10µm) will add to the externally applied bending stress creating further stress intensification resulting in further degradation of fatigue life.

In contrast, the compressive state of normal stress in Fe_4N white layer of thickness less than 10µm, will subtract from the externally applied bending stress resulting in reduction in stress intensification and increase in fatigue life.

To summarize, the findings of the FEM stress analysis carried out in the present study confirm and support the fatigue life versus white layer thickness correlation found in the experimental program carried out in this work.

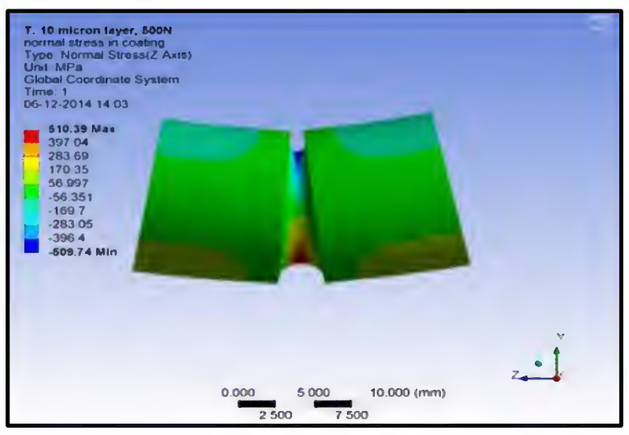

Fig. 7: Normal Fiber Stress in the Untreated Specimen

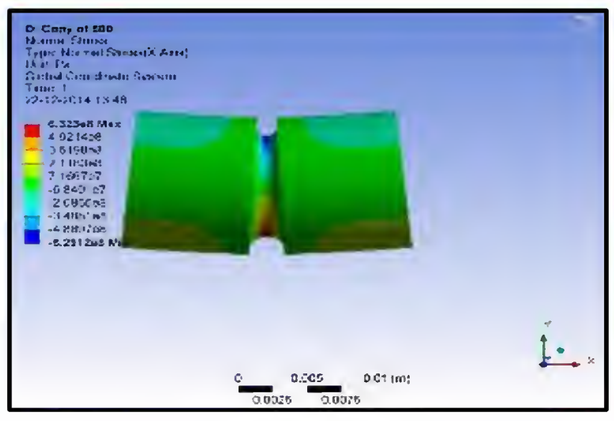

Fig. 8: Normal Fiber Stress in the Fe_4N White Layer of Thicknesses, T= 10 µm

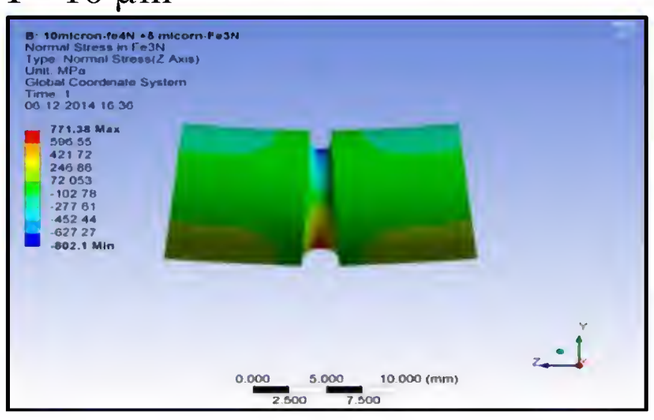

Fig. 9: Normal Fiber Stress in the $Fe_{2-3}N$ Layer of Composite White Layer of Thicknesses of T (Fe_4N) = 10 µm&T ($Fe_{2-3}N$) = 5 µm

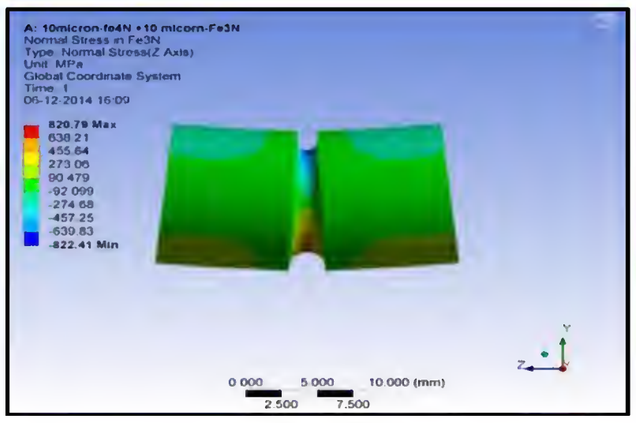

Fig. 10: Normal Fiber Stress in the $Fe_{2-3}N$ Layer in Composite Layer of Thicknesses of T(Fe_4N) = 10 µm + T ($Fe_{2-3}N$) = 10 µm

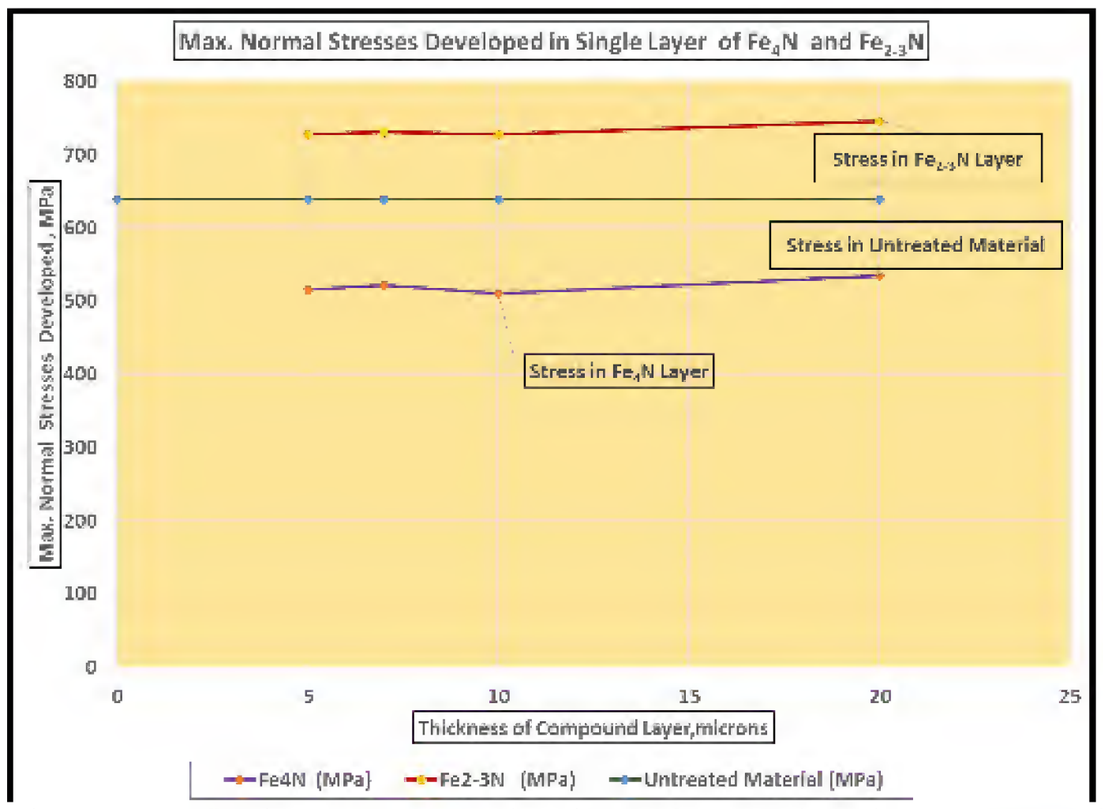

Fig. 11: Maximum Normal Fiber Stress in the Untreated Specimen and single layers of Fe_4N and $Fe_{2-3}N$

ISSN:2319-6890 (online),2347-5013(print)
1 Jan. 2017

Table 5.Max. Normal Stresses Developed in Single Layer of Fe_4N

Thickness of Layer, Microns	Max. Normal Stresses,MPa
0 (Untreated)	639.30
5	515.56
10	510.39
20	534.59

Table 6.Max. Normal Stresses Developed in Single Layer of $Fe_{2-3}N$ Layer

Thickness of Layer, Microns	Max. Normal Stresses, MPa
0 (Untreated)	639.30
5	727.64
10	728.03
20	746.32

Table 7: Max normal stresses developed in single layer of Fe_4N and compositewhite layer of $Fe_4N + Fe_{2-3}N$

Thickness of white layer, microns	Phases in white layer	Max normal stresses in Fe_4N (MPa)	Max normal stresses in $Fe_{2-3}N$ (MPa)
0 (Untreated)	Fe_4N	639.3	--
5	Fe_4N	515.56	--
10	Fe4N	510.39	--
15	Fe_4N (10 microns) & $Fe_{2-3}N$ (5 microns)	--	771.38
20	Fe_4N (10 microns) & $Fe_{2-3}N$ (10 microns)	--	820.79

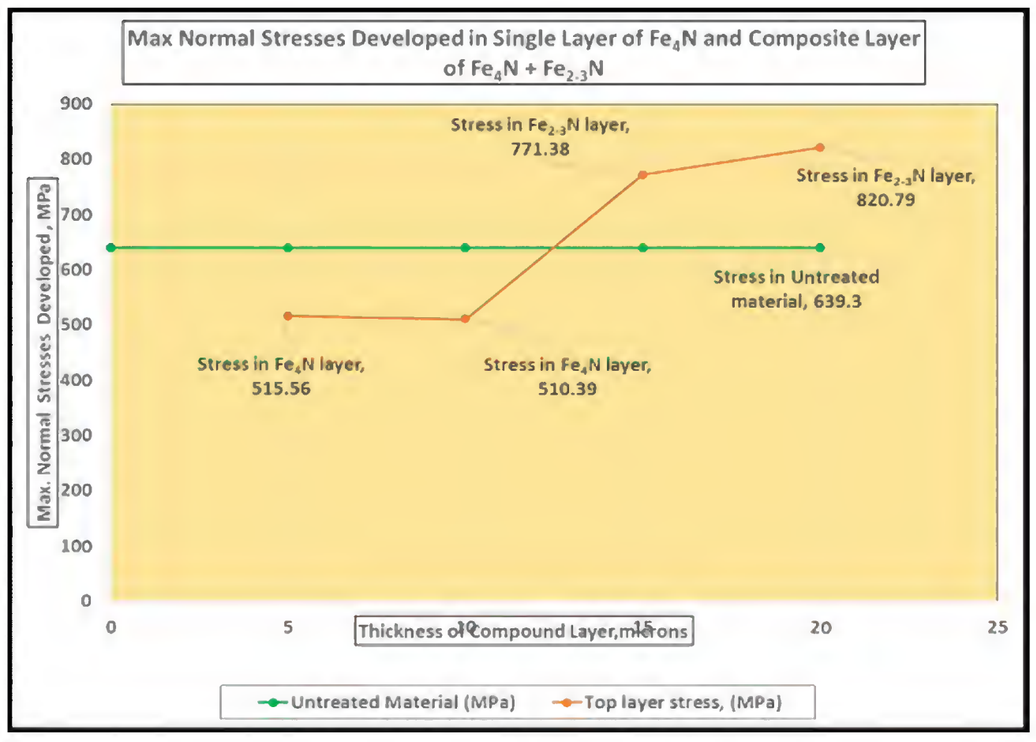

Fig. 12: Maximum Normal Fiber Stress in the Untreated Specimen, single layer of Fe_4N layer &composite layer of Fe_4N+$Fe_{2-3}N$

IV. Conclusions

i. FEA modelling reveals that up to a thickness of 10 µm of white layer the peak normal fiber stress is about 25% lower than the peak normal fiber stress in the base material.
ii. However, beyond a thickness of 10 µm, the stress in the white layer rapidly increases to 30% higher than the peak normal fiber stress in the base material. Lower the value of peak normal stress, better is the fatigue life of the material.
iii. The post- plasma nitriding residual stress in the white layer of $Fe_{2-3}N$ constitution is of tensile nature while that in the Fe_4N phase is of compressive nature.
iv. Presence of tensile normal stress in the $Fe_{2-3}N$ layer, (in white layer with thickness greater than 10µm) increases the outer fiber stress creating further stress intensification, resulting in degradation of fatigue life.
v. In contrast, the compressive nature of normal stress in Fe_4N white layer of thickness less than 10µm, lowers the outer fiber stress bending stress and results in reduction in stress intensification, helping in increasing the fatigue life.

Acknowledgement

We profusely thank the management of Electrical Research & Development Association (ERDA) for providing infrastructure facilities as well as for providing all required support during the research program. Our thanks also go out to all our colleagues in ERDA who extended their timely help, as and when required.

References

i. Metals Handbook, 8th Ed. American Society of Metals, Metals Park, Ohio, 1975.
ii. Steel and its heat treatment: Bofors handbook, Karl-Erik Thelning, Butterworth-Heinemann Limited
iii. Fatigue of metals. P. G. Forrest. Oxford 1962, Pergamon Press Ltd.
iv. Chang-Min Suh, Byung-Won Hwang, Ri-Ichi Murakami "Characteristics of Fatigue Crack Initiation and Fatigue Strength of Nitrided 1Cr-lMo-0.25V Turbine Rotor Steels", KSME International Journal, Vol, 16No. 8, pp. 1109--1116, 2002
v. S. Bhat and R. Patibandla, Metal Fatigue and Basic Theoretical Models: A Review, Alloy Steel - Properties and Use, Edited by Dr. Eduardo Valencia MoralesPublisherInTech Europe, December, 2011 pp.203-236
vi. Michael J. Schneider and Madhu S. Chatterjee, "Introduction to Surface Hardening of Steels", in Steel Heat Treating: Fundamentals and Processes, Volume 4A, ASM Handbook, American Society of Metals, Ohio, USA, (1996), p.395
vii. V. Rudnev, D. Loveless, R. Cook, and M. Black, Handbook of Induction Heating, Marcel Dekker, Inc., New York, (2003), p.777
viii. Gregory A. Fett. "Importance of Induction Hardened Case Depth in Torsional Applications', Heat Treating Progress, October (2009), pp.15-19
ix. Gerber, T. L., "Achievement of High Fatigue Resistance in Metals and Alloys", STP 476, American Society for Testing and Materials, Philadelphia, (1970), pp. 276-298.
x. Fuchs, H. O., "Analytical and Experimental Methods for Residual Stress Effects in Fatigue" STP 1004, American Society for Testing and Materials, Philadelphia, (1988), pp. 13-21
xi. Los Rios ER et al., "Fatigue crack initiation and propagation on shot-peened surfaces in 316 stainless steel". Int J Fatigue, Vol. 17, (1995), pp. 493–499

ISSN:2319-6890 (online),2347-5013(print)
1 Jan. 2017

xii. David K. Matlock, Khaled A. Alogab, Mark D. Richards, and John G. Speer, "Surface Processing to Improve the Fatigue Resistance of Advanced Bar Steels for Automotive Applications", Materials Research, Vol. 8, No. 4, (2005), pp. 453-459

xiii. Landgraf, R. W. and Chernenkoff. R. A., "Residual Stress Effects on Fatigue of Surface Processed Steels,", ASTM STP 1004, American Society for Testing and Materials, Philadelphia, (1988), pp.1-12

xiv. Cemal ÇARBOĞA, Kubilay KARACİF, and Burhanettin İNEM, "Effect of the Deformation of the Cold Drawing on Fatigue Life of the SAE 1010 Steel" Technology, Vol. 13, No. 1, (2010), pp.9-16

xv. ASM Handbook, Fatigue and Fracture, Vol. 19, ASM International, USA, (1996), p. 818

xvi. G. S. Junior, H.J.C. Voorwald, L. F. S. Vieira, M. O. H. Cioffi, and R.G. Bonora, "Evaluation of WC-10Ni Thermal Spray Coating with Shot Peening on the Fatigue Strength of AISI 4340 Steel", Procedia Engineering, Vol. 2, (2010), pp. 649-656

xvii. N.E. VivesDı´az, R.E. Schacherl, L.F. Zagonel, and E.J. Mittemeijer, "Influence of the Microstructure on the Residual Stresses of Nitrided Iron–Chromium Alloys", ActaMaterialia, Vol. 56, (2008), pp. 1196-1208

xviii. Thomas Grebmann, "Fe-C and Fe-N Compound Layers: Growth Kinetics and Microstructure", Dissertation an der, Universität Stuttgart, Bericht Nr. 206, September, (2007)

xix. Thomas R. Watkins, Roger D. England, Cheryl Klepser and N. Jayaraman, "Measurement and Analysis of Residual Stress in ε-Phase Iron Nitride Layers as a Function of Depth", Advances in X-ray Analysis,Vol.43, (2000), pp.31-38

xx. Z. Kolozswary, "Residual Stresses in Nitriding", Handbook of Residual Stress and Deformation of Steel", ASM International, (2002), pp. 209-219

xxi. Laurent Barrallier, Vincent Goret, Patrick Vardon and Dominique Deloison, "Residual Stresses and Distortion Simulation of Nitrided Disc", International Centre for Diffraction Data (2009), pp. 462-468

xxii. Tetsuya Takahashi, Jens Burghaus, Denis Music, Richard Dronskowski&Jochen M. Schneider, "Elastic properties of γ'-Fe_4N probed by nanoindentation and abinitio calculation", ActaMaterialia, Vol. 60, (2012), pp.2054-2060.